Oncogene (2020) 39:7127–7141
https://doi.org/10.1038/s41388-020-01484-9

ARTICLE

EZH2 overexpression dampens tumor-suppressive signals via an *EGR1* silencer to drive breast tumorigenesis

Xiaowen Guan[1,2,3] · Houliang Deng[1,2,3] · Un Lam Choi[1,2,3] · Zhengfeng Li[1,2,3] · Yiqi Yang[1,2,3] · Jianming Zeng[1,2,3] · Yunze Liu[1,2,3] · Xuanjun Zhang[1,2,3] · Gang Li[1,2,3]

Received: 24 September 2019 / Revised: 27 August 2020 / Accepted: 21 September 2020 / Published online: 2 October 2020

Abstract

The mechanism underlying EZH2 overexpression in breast cancer and its involvement in tumorigenesis remain poorly understood. In this study, we developed an approach to systematically identify the trans-acting factors regulating the EZH2 expression, and identified more than 20 such factors. We revealed reciprocal regulation of early growth response 1 (EGR1) and EZH2: EGR1 activates the expression of EZH2, and EZH2 represses EGR1 expression. Using CRISPR-mediated genome/epigenome editing, we demonstrated that EHZ2 represses EGR1 expression through a silencer downstream of the *EGR1* gene. Deletion of the *EGR1* silencer resulted in reduced cell growth, invasion, tumorigenicity of breast cancer cells, and extensive changes in gene expression, such as upregulation of GADD45, DDIT3, and RND1; and downregulation of genes encoding cholesterol biosynthesis pathway enzymes. We hypothesize that EZH2/PRC2 acts as a "brake" for EGR1 expression by targeting the *EGR1* silencer, and EZH2 overexpression dampens tumor-suppressive signals mediated by EGR1 to drive breast tumorigenesis.

Introduction

Polycomb repressor complex 2 (PRC2), which "writes" the epigenetic marks histone H3 lysine 27 di/tri-methylation (H3K27me2/3), acts as a transcriptional repressor. Additionally, PRC2 exerts a significant influence on the gene expression profiles of various cells, and thus participates in cell fate decisions and cell identity maintenance [1–3]. Increasing evidence shows that enhancer of zeste homolog 2 (EZH2), the catalytic subunit of PRC2, functions as an oncogene or tumor suppressor gene depending on the context. Gain-of-function mutations of *EZH2* have been found in different types of lymphomas, while loss-of-function mutations of *EZH2* have been found in T-cell acute lymphoblastic leukemia and diverse myeloid malignancies [4, 5]. Furthermore, *EZH2* was found to be the most significantly overexpressed epigenetic regulatory gene in solid tumors, e.g., in brain, breast, bladder, colon, gastric, kidney, lung, liver, ovarian, pancreatic, and prostate cancer [6–14].

EZH2 overexpression in cancers can be caused by *EZH2* amplification at the genomic level [15], or driven by transcription factors (TFs) such as MYC [16], E2F [17, 18], and STAT3 [19]. In addition, miRNAs targeting EZH2, such as miR-101, miR-26a, miR-98 [20–23], are downregulated in cancers. The interplay between the downregulation of these miRNAs and resulting upregulation of EZH2 is considered to establish a signal-amplification loop, resulting in sustained EZH2 overexpression [24]. In breast cancer, TFs such as FOXM1 [25], HIF1 [26], ELK1 [27], and SOX4 [28], and transcription coactivator ATAD2 [29] have been reported to regulate EZH2 expression. However, additional TFs regulating the expression of EZH2 in breast cancers remain to be found.

Research shows that knockdown of endogenous EZH2 inhibits cell proliferation, migration, and invasion in multiple cancer types, whereas overexpression of EZH2 leads to

Supplementary information The online version of this article (https://doi.org/10.1038/s41388-020-01484-9) contains supplementary material, which is available to authorized users.

✉ Gang Li
gangli@um.edu.mo

[1] Faculty of Health Sciences, University of Macau, Macau, China

[2] Cancer Centre, Faculty of Health Sciences, University of Macau, Macau, China

[3] Centre of Reproduction, Development and Aging, Institute of Translational Medicine, Faculty of Health Sciences, University of Macau, Macau, China

malignant transformation [23, 30, 31]. EZH2 was proposed to function as an oncogene through the silencing of the *INK4A–ARF* locus [32], E-cadherin [33], FOXC1 [34], as well as other suppressor loci. However, the mechanism underlying EZH2 oncogenic activity is not fully understood; adding to the complexity, EZH2 overexpression is considered by some researchers to be a consequence (passenger), instead of a driver, of tumorigenesis [35].

In this study, we developed an approach to systematically identify the TFs regulating the expression of EZH2 and demonstrate that early growth response 1 (EGR1) activates the expression of EZH2, which in turn represses the expression of EGR1 through a silencer region downstream of *EGR1*, in a PRC2-dependent manner. Upregulation of EGR1 resulting from the knockout of the silencer reduced tumorigenicity of breast cancer cells and elicited extensive changes in expression of genes involved in cell growth, death, migration, differentiation, and metabolism; therefore, we propose EZH2 govern a complex transcription program partly through the *EGR1* silencer to regulate diverse biological pathways, and thus dysregulation of EZH2 promotes breast tumorigenesis.

Results

Identification of trans-acting factors that regulate the expression of EZH2

To investigate the involvement of EZH2 in breast cancer, we first reanalyzed RNA-seq datasets of The Cancer Genome Atlas Breast Invasive Carcinoma (TCGA-BRCA) project. EZH2 was found to be overexpressed in most breast tumor samples, and strongly overexpressed in triple-negative (estrogen receptors (ER−), progesterone receptors (PR−), and Her2−) breast cancers (Fig. 1a). Luminal type A breast cancers have relatively lower expression of EZH2 compared with other subtypes, although the expression of EZH2 in this type of breast cancer is still significantly higher than in normal tissues. We hypothesized that there are unknown trans-acting factors regulating EZH2 in breast cancer. To identify these factors, we developed a data-mining approach (Fig. 1b). We first built a tool called *TFmapper* [36] that allows users to search across thousands of ChIP-seq datasets deposited in the Gene Expression Omnibus and reprocessed by *Cistrome* [37, 38]. Using this tool, we identified more than 50 trans-acting factors that bind the *EZH2* locus (Fig. 1c; Supplementary Table S1) in mammary glands. Next, we interrogated the RNA-seq datasets of the TCGA-BRCA, calculated pair-wise correlation coefficients between mRNA expression of EZH2 and candidate factors, and used $r > 0.3$ or $r < -0.3$ as the cutoffs to narrow down potential factors regulating EZH2 (Fig. 1c, Supplementary Table S2). The identification of more than 20 factors that satisfied these criteria indicates that EZH2 overexpression in breast cancers results from the dysregulation of multiple TFs. The previously reported EZH2 regulators, such as E2F1 [17] and FOXM1 [25], are among the factors identified by this approach, demonstrating the validity of our approach for identifying factors regulating a gene of interest. Interestingly, this analysis revealed that both ER and PR bind to the *EZH2* locus and their expression negatively correlates with the expression of EZH2, which is consistent with the high expression of EZH2 in triple-negative breast cancers.

We focused on one of the candidate EZH2 regulators, namely EGR1, for further analysis, because it has been shown that EGR1 directly activates multiple tumor suppressors [39, 40]. Furthermore, EGR1 is downregulated in breast cancer tissues compared with normal tissues (Fig. 1d) and its expression is negatively correlated with EZH2 expression (Fig. 1e). To extend the above observation, we analyzed mRNA and protein expression levels of EZH2 and EGR1 in normal breast epithelial cells (MCF-10A) and two human breast adenocarcinoma cell lines (MCF-7 and MDA-MB-231) (Supplementary Fig. S1a, b). The results showed that both breast cancer cell lines expressed higher levels of EZH2, but lower levels of EGR1, than the normal cell line. Next, we performed immunohistochemistry staining for EZH2 and EGR1 on tissue microarrays consisting of primary breast tumors and normal tumor-adjacent tissues (NAT). As shown in Supplementary Fig. S2, the protein levels of EGR1 in NAT were significantly higher than in tumor samples. Conversely, EZH2 was distinctly overexpressed in tumors compared with normal tissue. This result is consistent with the observation that EZH2 mRNA levels negatively correlate with EGR1 mRNA levels in RNA-seq datasets of TCGA-BRCA. It is noteworthy that both EGR1 and EZH2 were expressed at higher levels in Luminal B type tumors than in other types (Supplementary Fig. S2c), indicating that the mutual regulation of EZH2 and EGR1 reached a balance at a higher level in highly proliferative tumors. Considering that EGR1 binds to the *EZH2* promoter and a clear negative correlation between the expression of EZH2 and EGR1 was observed, we next sought to determine whether EGR1 represses the expression of EZH2.

EGR1 upregulates EZH2 expression

To investigate whether EGR1 regulates the expression of EZH2, the −1089 to +598 region of the *EZH2* transcription start site (TSS) was obtained by PCR amplification of human genomic DNA, and cloned into the promoter-less luciferase reporter vector pGL3-Basic. Surprisingly, co-transfection of

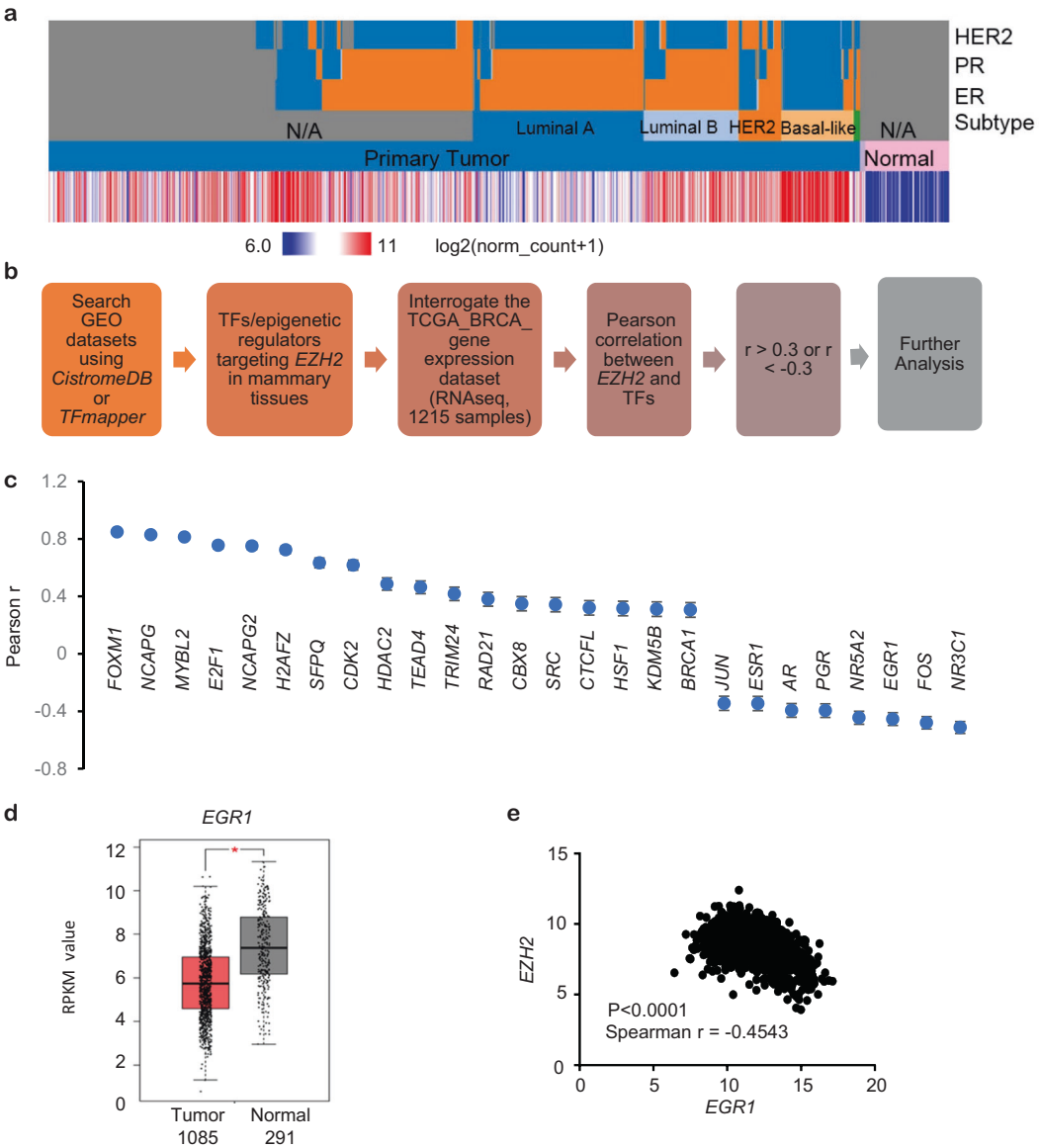

Fig. 1 The approach used to identify the transcription factors (TFs)/chromatin-binding proteins that regulate the expression of EZH2. a Heatmap of *EZH2* expression in breast normal tissue and tumor samples. RNA-seq data generated by the TCGA-BRCA (The Cancer Genome Atlas Breast Invasive Carcinoma) project were retrieved from the UCSC cancer genome browser. The dataset includes 1081 breast tumor samples and 134 normal breast tissue samples. The subtypes of the breast tumor samples are indicated. ER (estrogen receptor), PR (progesterone receptor), and HER2 statuses are color-coded, as follows: blue: negative, orange: positive, gray: not available or not applicable. **b** The approach used for identifying the transcription factors/epigenetic regulators targeting that regulate EZH2 transcription. **c** The RNA-seq dataset generated by the TCGA-BRCA was interrogated to calculate the correlation between the expression of *EZH2* and candidate EZH2 regulating factors. *FOXM1* forkhead box M1; *NCAPG* non-SMC condensin I complex subunit G; *MYBL2* MYB proto-oncogene like 2; *E2F1* E2F transcription factor 1; *NCAPG2* non-SMC condensin II complex subunit G2; *H2AFZ* H2A histone family, member Z; *SFPQ* splicing factor proline and glutamine rich; *CDK2* cyclin dependent kinase 2; *HDAC2* histone deacetylase 2; *TEAD4* TEA domain transcription factor 4; *TRIM24* tripartite motif containing 24; *RAD21* RAD21 cohesin complex component; *CBX8* chromobox 8; *SRC* NCOA1; nuclear receptor coactivator 1; *CTCFL* CCCTC-binding factor like; *HSF1* heat shock transcription factor 1; *KDM5B* lysine demethylase 5B; *BRCA1* BRCA1 DNA repair associated; *JUN* Jun proto-oncogene; AP-1 transcription factor subunit; *ESR1* estrogen receptor 1; *AR* androgen receptor; *PGR* progesterone receptor; *NR5A2* nuclear receptor subfamily 5 group A member 2; *EGR1* early growth response 1; *FOS* Fos proto-oncogene; *AP-1* transcription factor subunit; *NR3C1* nuclear receptor subfamily 3 group C member 1. Error bars indicate the 95% confidence intervals of each coefficient. **d** mRNA expression of EGR1 in breast cancer versus normal breast tissues. The data are retrieved from the RNA-Seq datasets of TCGA. The expression values are presented as Reads Per Kilobase of transcript per Million mapped reads (RPKM). **e** Spearman's rank correlation coefficient indicating a negative correlation between EZH2 and EGR1 mRNA levels in breast cancer tissues based on TCGA RNA-Seq data.

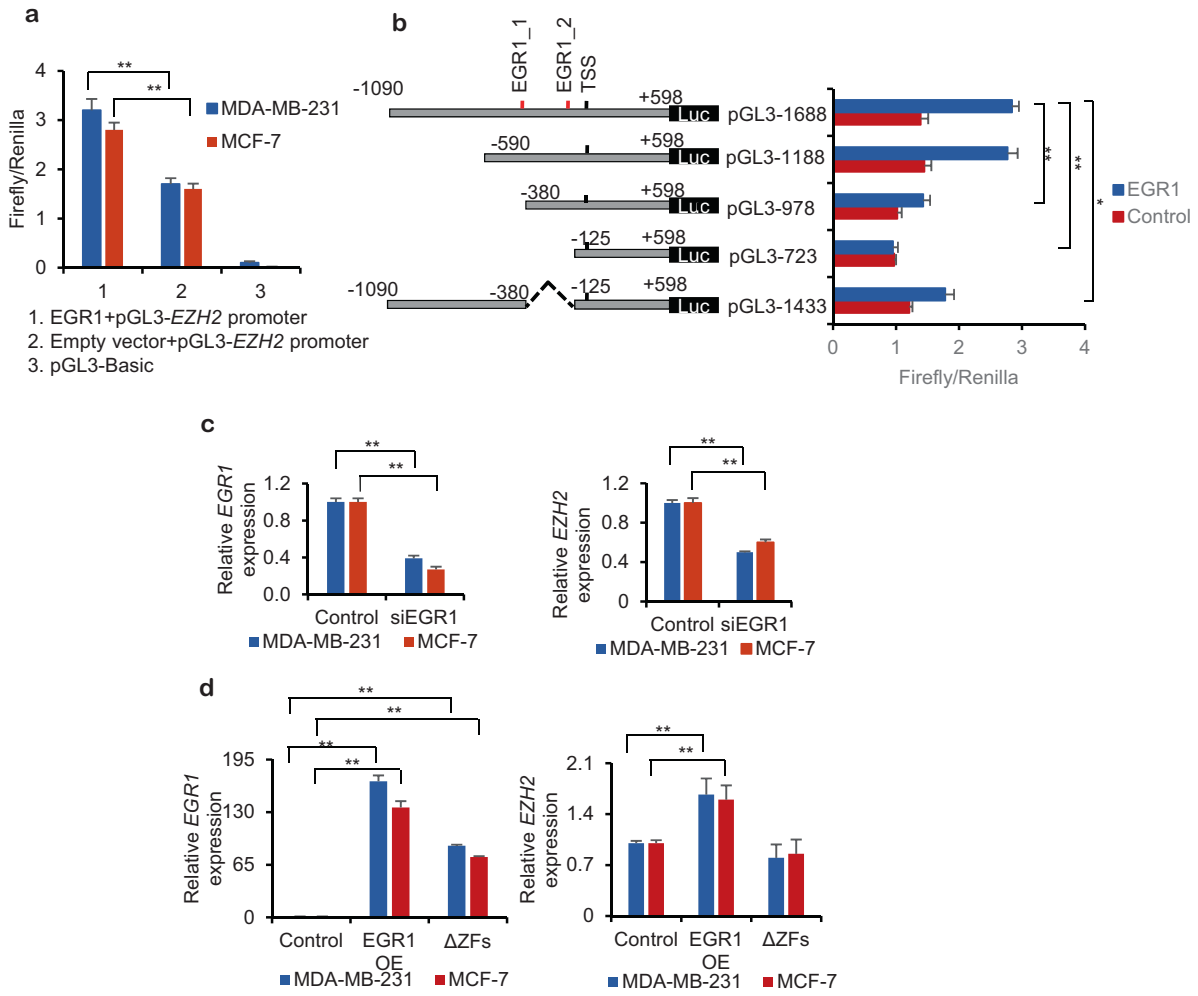

Fig. 2 EGR1 upregulates the expression of EZH2 in breast cancer cells. a EGR1 activated *EZH2* promoter luciferase activity. *EZH2* promoter (−1090 to +598 bp of *EZH2* transcription start site) was amplified from genomic DNA and cloned into the pGL3-basic vector. Firefly luciferase activity was determined by a dual luciferase assay system and normalized against the activity of *Renilla* luciferase. **b** pCMV6-EGR1 or the empty vector (control) was co-transfected into MCF-7 and MDA-MB-231 cells with a series of luciferase reporter constructs containing the full-length *EZH2* promoter or truncation/deletion variants of the *EZH2* promoter. The lengths of the promoters are indicated at the right. Firefly luciferase activity was determined by a dual luciferase assay system and normalized against *Renilla* luciferase activity. The putative EGR1 binding sites are indicated by red bars. **c** Knockdown of EGR1 by siRNA downregulates EZH2 expression. mRNA levels of EGR1 and EZH2 were examined by qRT-PCR; the results were normalized against values for GAPDH. **d** EGR1 overexpression upregulates EZH2 expression and the Cys2His2-type zinc finger domain plays a role in the regulation of EZH2 by EGR1. Unlike wild-type EGR1, Zinc finger-deleted (ΔZFs) elicited no significant effect on EHZ2. mRNA levels of EGR1 and EZH2 were examined by qRT-PCR, and the results were normalized against values for GAPDH. Bars represent mean ± SD of three biological replicates. $*P < 0.05$; $**P < 0.01$.

the reporter and EGR1 revealed that EGR1 activated the *EZH2* promoter luciferase reporter, instead of repressing it, in both MCF-7 or MDA-MB-231 cells (Fig. 2a). Moreover, EGR1 also activated the *EZH2* promoter luciferase reporter in normal breast epithelial cells (MCF-10A) (Supplementary Fig. S3a). Analysis of the *EZH2* promoter region by JASPAR [41] revealed that it contains two conserved EGR1 binding sites, at −399 to −380 bp, and at −149 to −129 bp of *EZH2* TSS (Supplementary Fig. S3b). Then, we performed ChIP-qPCR to validate EGR1 binding at the two sites in MDA-MB-231, MCF-7, and MCF-10A cell lines. As shown in Supplementary Fig. S3c, EGR1 was enriched at both binding sites in all cell lines. Through a series of truncation/deletion analyses (Fig. 2b), we found that the proximal region of the *EZH2* promoter (−590 to +598 bp of the TSS of EZH2) retains most of the activity of the full-length *EZH2* promoter. However, deletion of either of the regions harboring the EGR1 binding sites resulted in decreased promoter activity and EGR1 responsiveness. Deletion of both EGR1 binding sites resulted in total loss of EGR1 responsiveness, suggesting the involvement of EGR1 and the

corresponding EGR1 binding sites in regulating the activity of the *EZH2* promoter. Further, knockdown of EGR1 in both MCF-7 and MDA-MB-231 cells resulted in downregulation of EZH2, while overexpression of EGR1 led to the opposite effect (Fig. 2c, d). EGR1 contains a highly conserved DNA-binding domain composed of three zinc fingers [42]. To test if the DNA-binding domain plays a role in the regulation of EZH2 by EGR1, we generated a construct replacing the three zinc fingers with a flexible glycine-serine linker (GGGGS × 3). Next, we transfected the construct into MCF-7 and MDA-MB-231 cells. The results indicated that EZH2 expression did not change (Fig. 2d), showing that the DNA-binding domain of EGR1 is indispensable in the regulation of EZH2 by EGR1. In addition, EGR1 has been shown to interact with CREB-binding protein (CBP) and p300 [43]. However, the ability of EGR1 to up-regulate EZH2 expression was not markedly compromised in CBP or p300 knockdown cells (Supplementary Fig. S4), suggesting additional proteins might mediate the function of EGR1. Taken together, these results indicate EGR1 stimulates the expression of EZH2.

EZH2 represses EGR1 expression in a PRC2-dependent manner

The observed activation of EZH2 by EGR1 contrasts with the negative correlation between the expression of EZH2 and that of EGR1 in the TCGA-BRCA datasets. Therefore, we hypothesize that EZH2 exerts an inhibitory effect on EGR1 expression. To test this hypothesis, we manipulated the expression of EZH2 in MCF-7 cells and MDA-MB-231 cells. Knockdown of EZH2 in both cell lines resulted in EGR1 upregulation at both mRNA and protein levels, while overexpression of EZH2 decreased the expression of EGR1 in both cell lines (Fig. 3a, b), indicating EZH2 negatively regulates the expression of EGR1. There are several lines of evidence suggesting that EZH2 might function independently of PRC2 and its histone methyltransferase activity in certain cellular contexts. To test whether the inhibition of EGR1 expression by EZH2 depends on PRC2 and its histone methyltransferase activity, we first mutated the catalytic site of EZH2 (Y726F) and transfected the two cell lines with EZH2-Y726F, the silencing effects of EZH2 on EGR1 were diminished (Fig. 3b). Next, we treated MCF-7 cells and MDA-MB-231 cells with the EZH2 inhibitor EPZ-6438. EGR1 was dramatically upregulated by EPZ-6438 treatment (Fig. 3c). Further, we used three different siRNAs to knockdown embryonic ectoderm development (EED), one of the core components of PRC2, in MCF-7 cells and MDA-MB-231 cells. The results demonstrated that EED knockdown caused a significant upregulation of EGR1 expression (Fig. 3d). Further, after EED knockdown, the ectopic expression of EZH2 was found to no longer down-regulate EGR1 expression in MCF-7 cells and MDA-MB-231 cells (Fig. 3e). To examine whether the repression of EGR1 by EZH2 is conserved in other cell types, we knocked out EED in C2C12 cells using the CRISPR-Cas9 system and found that EGR1 was significantly increased in EED-null C2C12 cells. Furthermore, EZH2 could not suppress EGR1 expression in EED-null C2C12 cells (Supplementary Fig. S5). Together, these results suggest that EZH2 represses EGR1 expression in a PRC2-dependent manner.

Identification of a distal silencer braking the expression of EGR1

To determine how EZH2 represses the expression of EGR1, we examined the epigenetic settings at the *EGR1* locus using the ENCODE ChIP-seq datasets of MDA-MB-231 and MCF-7 cells. Unexpectedly, we found that there is no H3K27me3 mark at the *EGR1* promoter region. However, there are significant peaks of H3K27me3 spanning 2.9 kb, 26 kb downstream of the *EGR1* TSS. The area harboring H3K27me3 is also marked by pronounced peaks of H3K4me1, as well as peaks of H3K27ac and H3K4me3 (Fig. 4a; Supplementary Fig. S6a). We hypothesized that this area represents a distal regulatory element of *EGR1*. To test the hypothesis, we first performed ChIP-qPCR to validate the status of the histone marks and EZH2 binding at the +26 kb locus of *EGR1* in both cell lines. We divided the area into three sub-regions: Regulatory region 1 (R1), Regulatory region 2 (R2), and Regulatory region 3 (R3) (Fig. 4a). As shown in Fig. 4b and Supplementary Fig. S6b, H3K4me3 and H3K4me1 were enriched at R2, whereas H3K27me3 was enriched at R1 and EZH2 binding was detected in all three regions. Next, we cloned these three sub-regions individually into the pGL3 promoter luciferase reporter and assayed their activities. As shown in Fig. 4c, R1 inhibits the luciferase activity of the pGL3 promoter luciferase reporter, suggesting that it functions as a silencer element.

To determine whether EZH2 represses the expression of EGR1 through this distal regulatory region, we fused the catalytically inactive mutant Cas9 (dCas9) with EZH2 by Gibson assembly and generated constructs encoding sgRNAs targeting the different sub-regions (R1, R2, and R3). In both MCF-7 and MDA-MB-231 cells, the dCas9/EZH2 fusion protein directed by all three sgRNAs repressed the expression of EGR1 (Fig. 4d); among them, the sgRNA targeting Region 1 had the strongest effect, consistent with the luciferase reporter results. Next, we knocked out a 1780 bp segment from this distal regulatory region using the CRISPR/Cas9 mediated method and obtained multiple clones containing a heterozygous deletion of the segment in both MCF-7 and MDA-MB-231

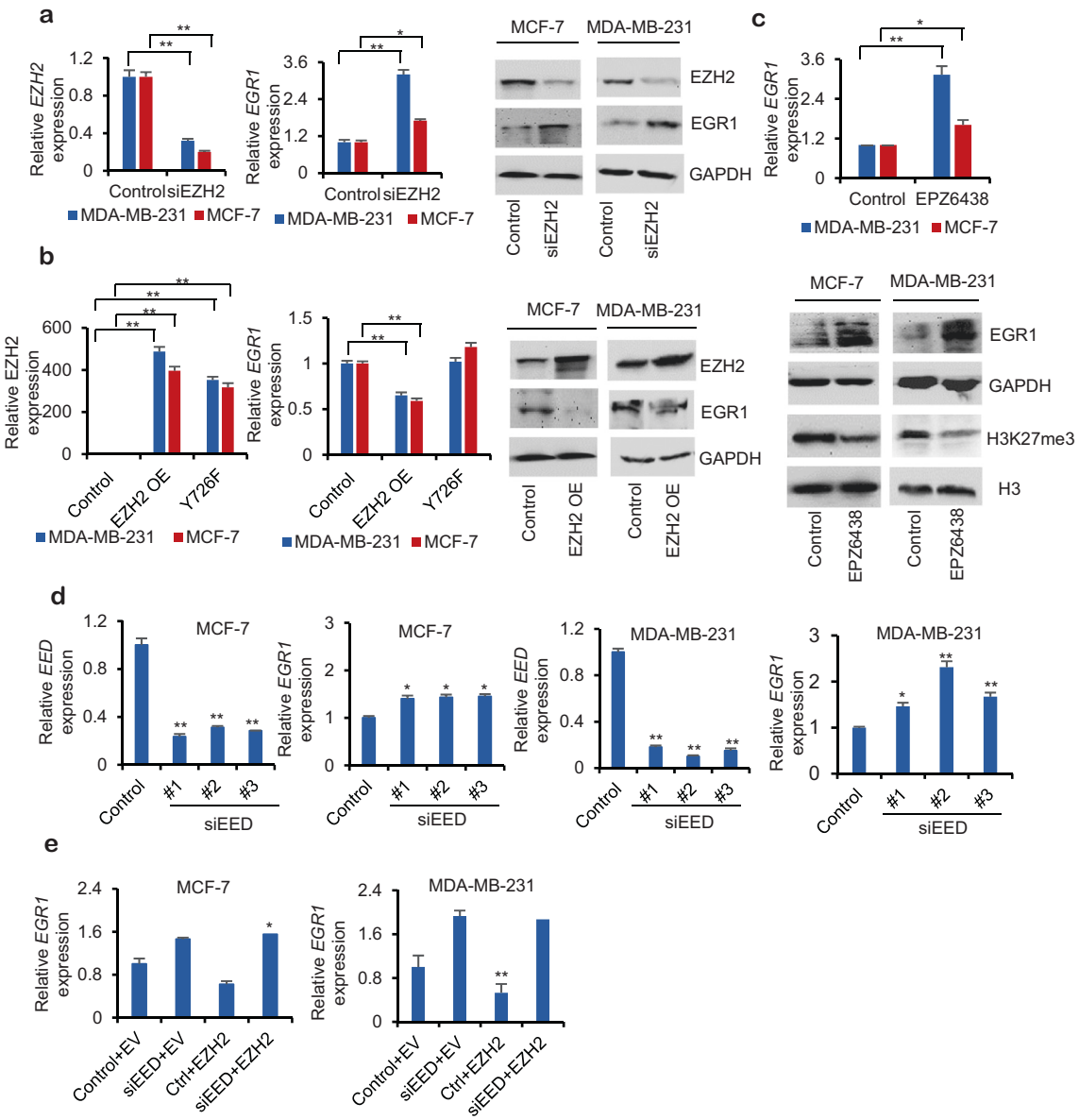

Fig. 3 EZH2 represses EGR1 expression in a PRC2-dependent manner in breast cancer cells. a Knockdown of EZH2 by siRNA results in the upregulation of EGR1 expression in MCF-7 and MDA-MB-231 cells. mRNA levels of EGR1 and EZH2 were examined by qRT-PCR (left panels) and protein levels of EGR1 and EZH2 were examined by western blot analysis (right panel). GAPDH was used as the loading control. **b** Repression of EGR1 by EZH2 is dependent on the catalytic activity of PRC2. The pcDNA3.2/GW/D-TOPO plasmids encoding wild-type EZH2 or catalytic-dead EZH2 (Y726F, tyrosine 726 to phenylalanine mutation) were transfected into cells. mRNA levels of EGR1 and EZH2 were examined by qRT-PCR (left panels) and protein levels of EGR1 and EZH2 were examined by western blot analysis (right panel). GAPDH was used as the loading control. **c** Treatment with EZH2 inhibitor upregulates EGR1 expression. MCF-7 cells and MDA-MB-231 cells were treated with 50 nM EPZ-6438 for 48 h. Upper panel: mRNA levels of EGR1 were examined by qRT-PCR. Lower panel: protein levels of EGR1 and the levels of H3K27me3 were examined by western blot analysis, GAPDH and histone H3 were used as loading controls. **d** Knockdown of EED upregulates EGR1 expression. MCF-7 cells and MDA-MB-231 cells were transfected with siRNAs against EED for 48 h; mRNA levels of EGR1 were examined by qRT-PCR. **e** The inhibition of EGR1 by EZH2 requires EED. MCF-7 and MDA-MB-231 cells were first transfected with the most effective EED siRNA for 24 h, and then transfected with EHZ2 or empty vector (EV) for 48 h; mRNA levels of EED and EGR1 were examined by qRT-PCR. All the qRT-PCR results were normalized against values for GAPDH. Error bars represent mean ± SD of three independent experiments performed in triplicate. $*P < 0.05$, $**P < 0.01$.

cells (Fig. 4e; Supplementary Figs. S7 and S8). In these clones, upregulation of EGR1 expression was observed (Fig. 4e), further supporting that EGR1 is regulated by this region, which is named the $EGR1^{+26\,kb}$ silencer. To ascertain that the $EGR1^{+26\,kb}$ silencer is involved in the repression of EGR1 by EZH2, we transfected EZH2 into

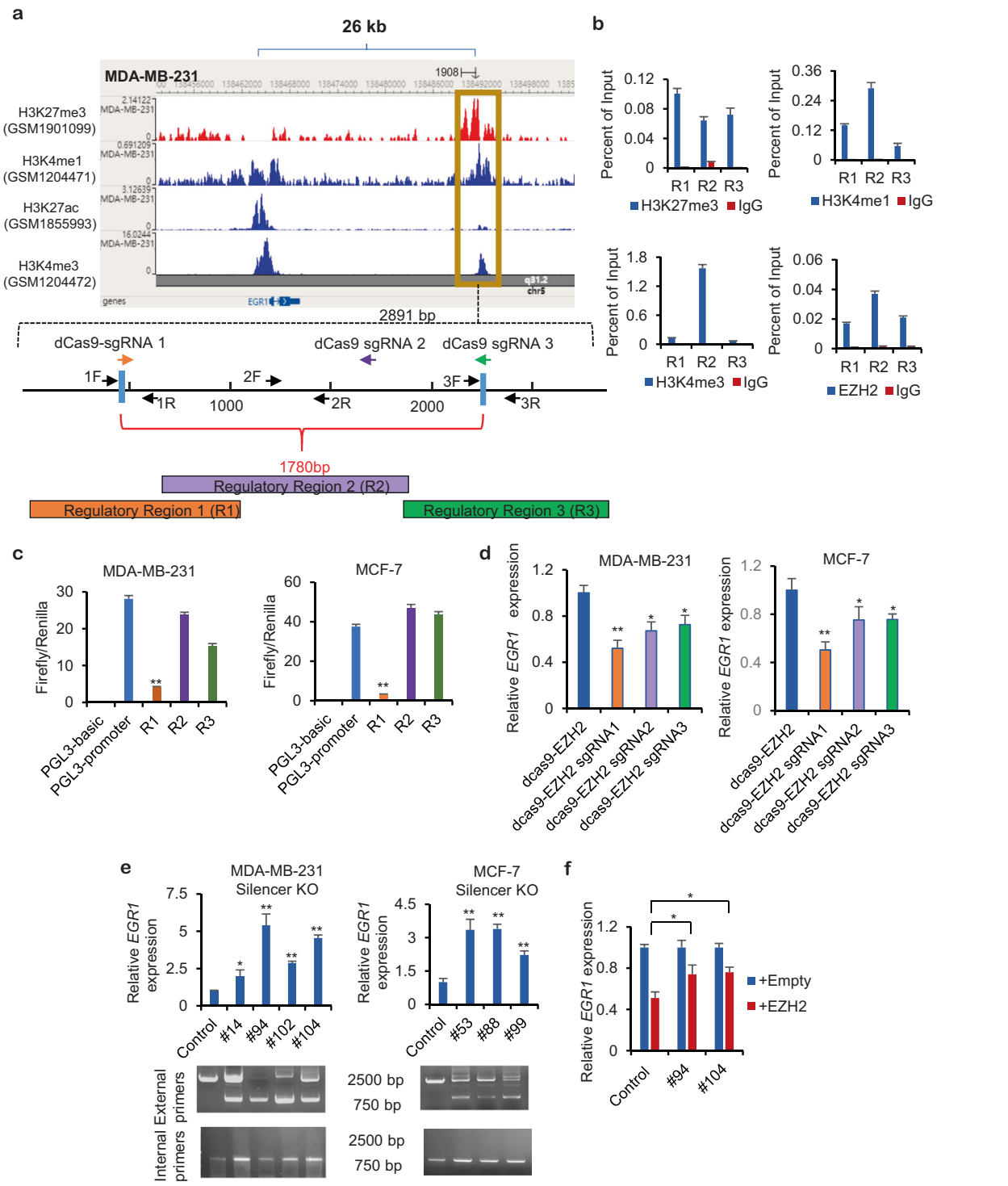

MDA-MB-231 wild-type and *EGR1*$^{+26\,kb}$ silencer-knockout (silencer KO) cells, and found that the silencing effects of EZH2 on EGR1 were partially diminished in two independent silencer-KO clones (Fig. 4f). Taken together, these results suggest that EZH2 represses EGR1 expression through a silencer 26 kb downstream of its TSS. By examining the publicly available datasets, we noted that H3K27me3 peaks around 26 kb downstream of *EGR1* TSS are present in multiple immortalized cell lines, embryonic stem cells, stem cell-derived neuroectoderm and endoderm cells, as well as primary cells and tissues (Supplementary Fig. S9), suggesting that this putative *EGR1* silencer element might be conserved across different cell types.

◀ **Fig. 4 Identification of a distal silencer that represses the expression of EGR1. a** Upper panel: the ChIP-seq datasets of histone marks in MDA-MB-231 cells deposited in the Gene Expression Omnibus (GEO) of NCBI, including those for H3K27me3, H3K4me1, H3K27ac, and H3K4me3, were reprocessed by the *Cistrome* Project and retrieved through *TFmapper*. The epigenomic data at the *EGR1* locus were visualized through the WashU Epigenome Browser, and the corresponding accession numbers are indicated at the left. The putative regulatory region (2891 bp) of *EGR1* is highlighted by the gold rectangle; Lower panel: the schematic under the dashed brace depicts the three sub-regions of the distal EGR1 regulatory element, R1, R2, and R3. The locations of the ChIP primers for each putative regulatory sub-region of EGR are indicated by arrows in the panel. **b** ChIP-qPCR analyses of H3K27me3, H3K4me1, H3K4me3, and EZH2 at the *EGR1* loci in MDA-MB-231 cells. The results are shown as percentages of the input chromatin DNA. Error bars represent mean ± SD of triplicates. **c** Activities of the sub-regions of the putative silencer were assessed by luciferase reporter assays ($n = 3$) in MCF-7 and MDA-MB-231 breast cancer cells. **d** MCF-7 cells and MDA-MB-231 cells were transfected with dCas9-EZH2-sgRNAs or dCas9-EZH2. After 48 h, mRNA levels of EGR1 were examined by qRT-PCR and the results were normalized against the levels of GAPDH. The locations of sgRNAs targeting sub-regions of the regulatory element are indicated by arrows. **e** Deletion of the $EGR1^{+26\,kb}$ silencer results in upregulation of EGR1. Upper panel: deletion of the *EGR1* silencer was achieved by a CRISPR-Cas9 mediated method. The locations of sgRNAs used are indicated by the blue vertical bars. mRNA levels of EGR1 were examined by qRT-PCR, and the results were normalized against data for GAPDH. Lower panel: Gel images showing PCR amplification of genomic DNA using primers outside and inside the putative silencer region. **f** Deletion of the *EGR1* silencer results in diminished silencing effect of EZH2 on EGR1. EZH2 or empty vector (EV) were transfected into parental cells or cells with a heterozygous deletion of EGR1 silencer (#94, #104). mRNA levels of EGR1 were examined by qRT-PCR 48 h after transfection, and the results were normalized against values for GAPDH. Error bars represent mean ± SD of at least three experimental replicates. $*P < 0.05$; $**P < 0.01$.

Deletion of the $EGR1^{+26\,kb}$ silencer inhibits the tumorigenic phenotype of breast cancer cells in vitro and in vivo

Next, we examined the effects of deleting the $EGR1^{+26\,kb}$ silencer on the tumorigenic phenotype of breast cancer cells. Deletion of the silencer region of *EGR1* in MDA-MB-231 cells resulted in significant impairment of cell proliferation (Fig. 5a) and colony formation ability (Fig. 5b). Flow cytometry analysis revealed that more cells were stuck in cell cycle, particularly in G0/G1 phase, upon deletion of the silencer as compared to control cells (Fig. 5c). Furthermore, deletion of the silencer region of EGR1 in MCF-7 cells also resulted in cell growth retardation (Supplementary Fig. S10a–c). In addition, cell migration and invasion were also impaired upon the deletion of the silencer in MDA-MB-231 cells (Fig. 5d). To further validate the role of the $EGR1^{+26\,kb}$ silencer in vivo, we inoculated MDA-MB-231 and MCF-7 wild-type cells and $EGR1^{+26\,kb}$ silencer-KO cells into female nude mice subcutaneously. The tumors formed in the silencer-KO group showed substantially slower growth than those in the wild-type group (Fig. 5e and Supplementary Fig. S10d). Moreover, at the end of the experiment, the tumors were significantly smaller in the silencer-KO groups than in the control groups of both MDA-MB-231 (Fig. 5f, g) and MCF-7 cells (Supplementary Fig. S10e, f). These in vivo findings concur with the in vitro data, collectively demonstrating that deletion of the $EGR1^{+26\,kb}$ silencer inhibits the tumorigenic phenotype of breast cancer cells suggesting an involvement in EHZ2-mediated breast tumorigenesis.

Changes in gene expression in the $EGR1^{+26\,kb}$ silencer-knockout cells

Next, we performed RNA-seq analysis of wild-type and silencer-KO MCF-7 and MDA-MB-231 cells, and found that deletion of the $EGR1^{+26\,kb}$ silencer led to extensive changes in gene expression. As in MCF-7 cells, after the silencer was knocked out, the expression of 5165 genes was altered by 1.4-fold or more ($\log_2$ FC > 0.49, adjusted P value < 0.05), with 2209 genes upregulated and 2956 downregulated. Similarly, the expression of 1125 genes was altered by more than 1.4-fold in MDA-MB-231 cells, with 544 genes upregulated and 581 downregulated after the silencer was knocked out (Fig. 6a). Among these, changes in the expression of a common set of 255 genes between the two cell lines were found following silencer deletion, with 117 genes upregulated, and 138 downregulated in both cell lines (Fig. 6b). Gene ontology (GO) analysis revealed that the commonly upregulated genes were enriched in biological processes such as "intrinsic apoptotic signaling pathway," "tissue development," and "cell differentiation." The downregulated genes were enriched in biological processes such as "semaphorin-plexin signaling pathway," "positive regulation of cell population proliferation," "regulation of cell migration" (Fig. 6c, d).

GO analysis also revealed that EGR1 has a complex effect on metabolism—the commonly upregulated genes in *EGR1* silencer-KO cells were enriched in both GO terms of "negative regulation of metabolic process" and "positive regulation of metabolic process." While downregulated genes were enriched in GO terms related to biosynthetic processes, particularly the synthesis of cholesterol, sterols, and lipids (Fig. 6d). Specifically, SLC27A2 (solute carrier family 27 member 2), which functions as an acyl-coenzyme A (CoA) synthetase, and thereby participates in the synthesis of complex lipids and oxidation of fatty acids, was upregulated more than 2-fold (Supplementary Fig. S11). Most notably, multiple genes encoding cholesterol biosynthesis pathway enzymes, including 3-hydroxy-3-methylglutaryl-CoA synthase 1 (HMGCS1), farnesyl diphosphate synthase (FDPS), isopentenyl-diphosphate

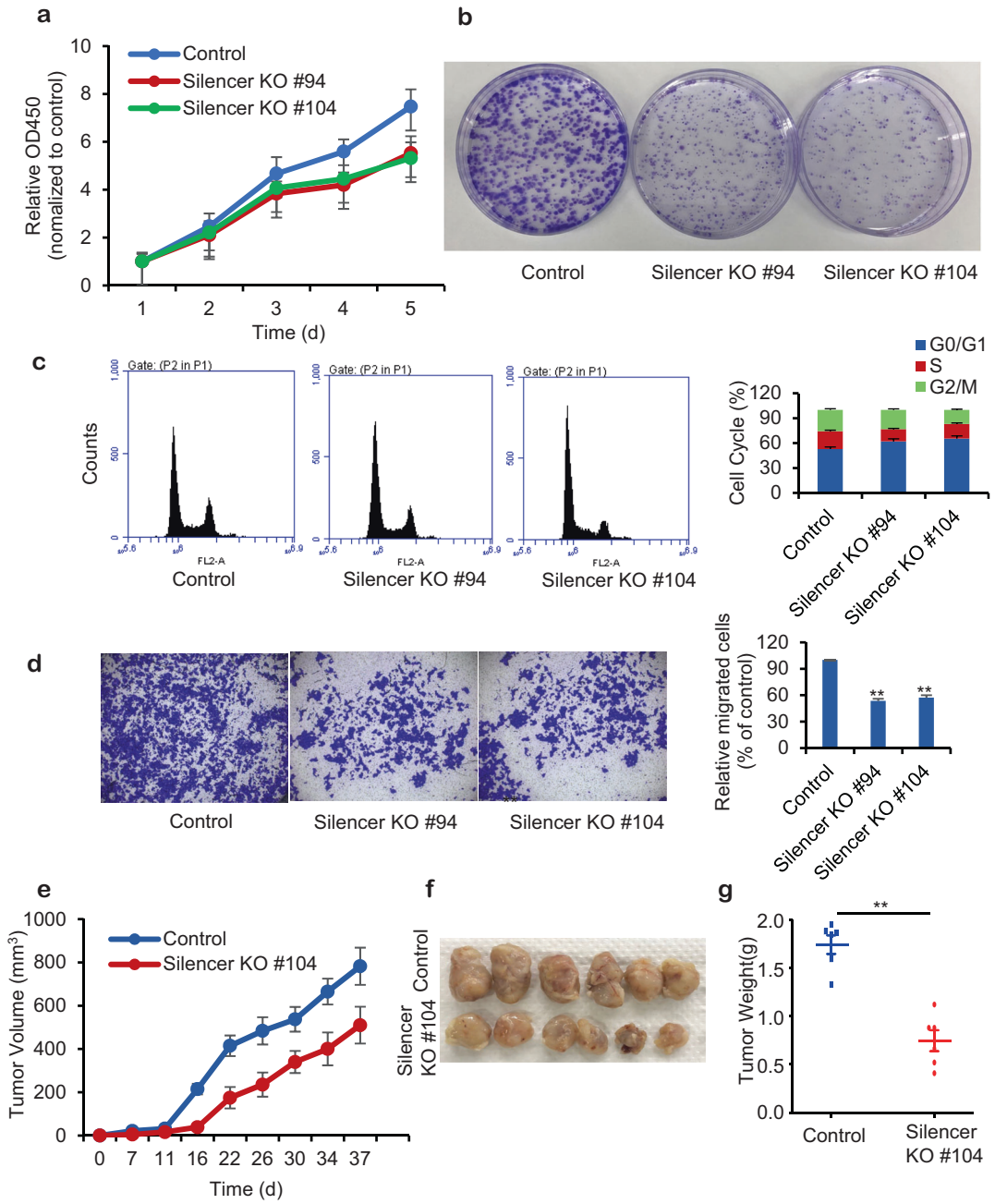

Fig. 5 Deletion of the EGR1$^{+26\,kb}$ silencer region represses the tumorigenic phenotype of MDA-MB-231 cells in vitro and in vivo. **a** Parental (Control) MDA-MB-231 cells or two independent *EGR1* silencer-knockout clones (Silencer KO #94 and #104) were seeded into a 96-well plate, and cell growth was measured with the CellTiter-Glo® Luminescent Cell Viability Assay (Promega). **b** Parental (Control) MDA-MB-231 cells or the *EGR1* silencer-knockout (Silencer KO #94 and #104) cell lines were cultured for 10 days, followed by 0.5% crystal violet staining to examine the effects of knocking out the *EGR1* silencer on colony formation. **c** Cell cycle analysis was performed via flow cytometry after staining the cells with propidium iodide. Left 3 panels, representative cell cycle profiles. Right panel, the quantitative measurements of cell cycle phases. **d** Transwell assays were performed to evaluate the effects of *EGR1* silencer knockout on cell migration and invasion. Left panel, representative images of transwell assays. Right panel, quantitative analysis of the migration rates. Error bars represent mean ± SD of three experimental replicates. $^{**}P < 0.01$. **e**–**g** Parental (Control) MDA-MB-231 cells or *EGR1* silencer-knockout (Silencer KO) clones #104 were subcutaneously inoculated into nude mice. Tumor volumes were calculated using the formula $V = (a \times b^2)/2$, in which "*a*" is the longest and "*b*" is the shortest diameter of the tumor (**e**). Data are mean ± SD; $n = 6$. At the end of the experiment, tumors were dissected out (**f**) and weighed (**g**). Statistical differences were determined using Student's *t* test. $^{*}P < 0.05$; $^{**}P < 0.01$.

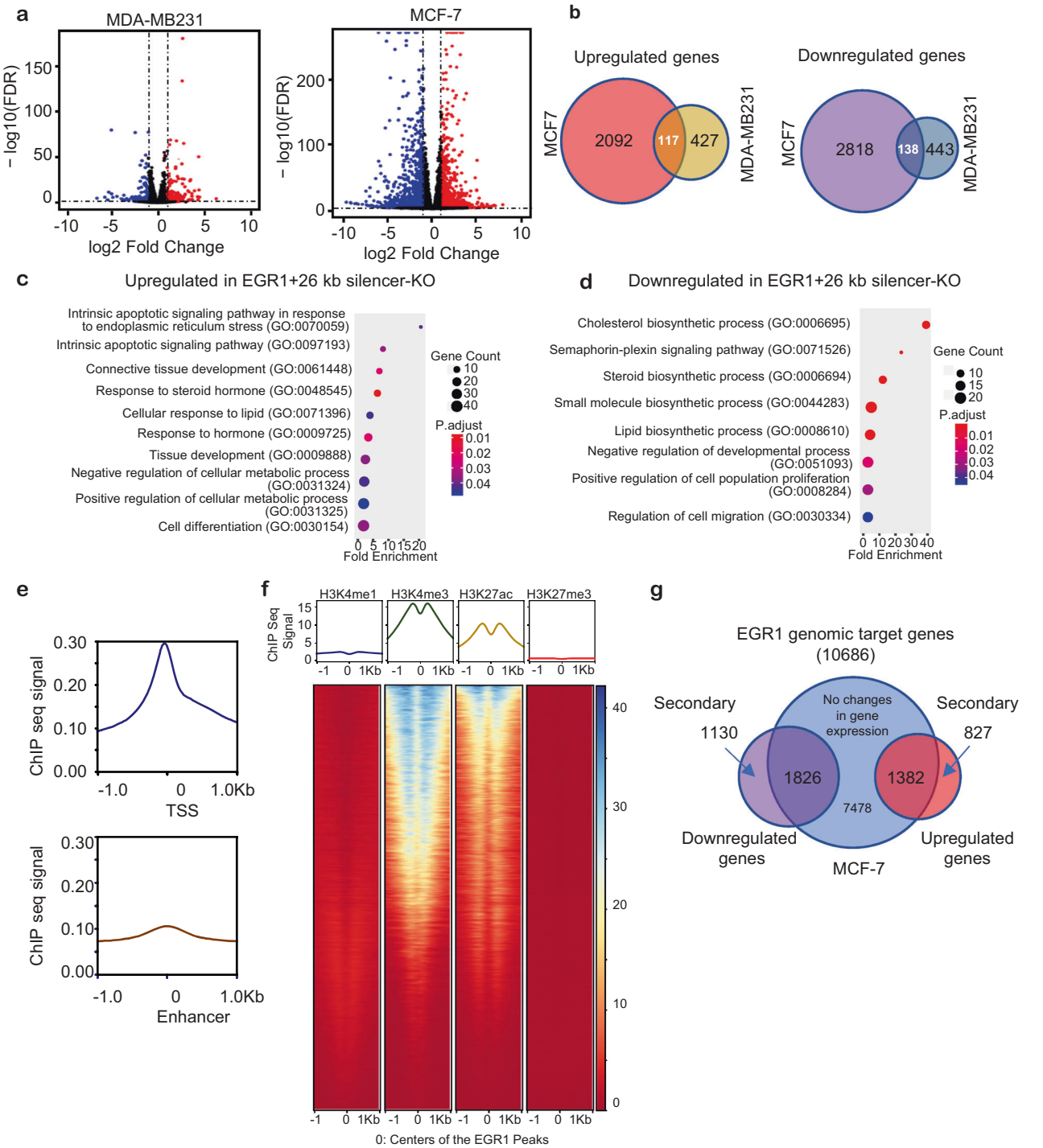

Fig. 6 Extensive changes in gene expression in EGR1$^{+26\,kb}$ silencer-knockout cells. a RNA-seq was performed to examine the effects of knocking out the +26 kb silencer of *EGR1* in MCF-7 and MDA-MB-231 cells. The volcano plot shows statistical significance ($-\log_{10}$ (adj *P* value)) plotted against $\log_2$ fold change of genes for silencer-knockout cells against parental cells. Differentially expressed genes were selected based on criteria of adjusted $P < 0.05$ and absolute $\log_2$ fold change > 0.49. **b** Venn diagrams of overlapping and unique genes downregulated or upregulated as a result of the silencer knockout in MDA-MB-231 and MCF-7 cells. **c** Gene ontology analysis of commonly downregulated or upregulated genes in the *EGR1*$^{+26\,kb}$ silencer-KO MDA-MB-231 and MCF-7 cells compared to wild-type cells. **d** Normalized reads coverage of EGR1 around transcriptional start sites (TSS) and centers of enhancers in MCF-7 cells. The ChIP-seq dataset (GSM1010844) for EGR1 was retrieved from Gene Expression Omnibus (GEO) and reprocessed. Enhancers in MCF-7 cells were defined according to histone modification patterns from reference epigenome series ENCSR247DVY. **e** Normalized reads coverage of histone modifications at the ±1 kb region flanking EGR1 peak center. Bottom panels show heatmap representations of normalized read density of H3K4me1, H3K4me3, H3K27ac, and H3K27me3. **f** Venn diagram of overlap between EGR1 target genes and genes differentially expressed in *EGR1*$^{+26\,kb}$ silencer-KO cells (>1.4-fold, $P < 0.05$).

delta isomerase 1 (IDI1), mevalonate diphosphate decarboxylase (MVD), 7-dehydrocholesterol reductase (DHCR7), lanosterol synthase (LSS), and squalene epoxidase (SQLE), were downregulated in both types of *EGR1* silencer-KO cells (Supplementary Fig. S12 and Table S3).

Next, we examined the upregulated genes that contribute to the enrichment in "intrinsic apoptotic signaling pathway." We found DNA-damage inducible transcript 3 (DDIT3) was upregulated more than twofold in both types of *EGR1* silencer-KO cells (Supplementary Fig. S11). DDIT3 encodes C/EBP Homologous Protein (CHOP), as a TF, CHOP plays a pivotal role in endoplasmic reticulum stress-induced apoptosis [44, 45]. Two known targets of CHOP, protein phosphatase 1 regulatory subunit 15A (*PPP1R15A*), also called *GADD34*, and tribbles pseudokinase 3 (*TRIB3*) [46, 47], were also found to be induced in the *EGR1* silencer-KO cells (Supplementary Fig. S11), suggesting the activation of DDIT3 mediated pathway. Examination of EGR1 ChIP-seq data in MCF-7 cells revealed the promoter of *DDIT3* harbors a significant EGR1 binding peak (Supplementary Fig. S13), suggesting EGR1 potentially activates DDIT3 expression directly. To be noted, both *PPP1R15A* and *TRIB3* also harbor EGR1 binding peaks (Supplementary Fig. S13), suggesting their upregulation could be due to the combined effects of EGR1 and DDIT3. Also, Rho Family GTPase 1 (RND1), which inhibits cell migration by promoting disassembly of actin filaments [48], and suppresses mammary tumorigenesis and epithelial–mesenchymal transition by restraining Ras-MAPK signaling [49], was upregulated more than twofold in both types of *EGR1* silencer-KO cell lines (Supplementary Fig. S11). Significantly, *RND1* also harbors a significant EGR1 binding peak (Supplementary Fig. S13), suggesting *RND1* is a direct target gene of EGR1. To gain more insights into how upregulation of EGR1 resulted in delayed cell growth in *EGR1* silencer-KO cells, we performed gene set enrichment analysis using the gene matrix of the Kyoto Encyclopedia of Genes and Genomes cell cycle (hsa04110) (Supplementary Fig. S14a). Although no significant enrichments were discovered, we found all three growth arrest and DNA-damage inducible (*GADD45*) genes were upregulated in both types of *EGR1* silencer-KO cells (Supplementary Fig. S14b). Independent RT-PCR analysis found that GADD45B was the dominant form of GADD45 in both MCF-7 and MDA-MB-231 (Supplementary Fig. S14c) and further validated the upregulation of GADD45 in *EGR1* silencer-KO cells (Supplementary Fig. S14d). Examination of EGR1 ChIP-seq data revealed the promoters of all three *GADD45* genes harbored significant EGR1 binding peaks (Supplementary Fig. S14e), indicating *GADD45* genes are bona fide EGR1 target genes.

To investigate why the upregulation of EGR1 led to extensive changes in gene expression, we reanalyzed the ChIP-seq dataset for EGR1 in MCF-7 cells [50]. The binding signals of EGR1 to promoters are much stronger than those to enhancers (Fig. 6e). We next calculated the intensities of multiple histone modifications with reference to the center of EGR1 peak. We found that EGR1 binding sites are associated with strong H3K4me3 and H3K27ac signals, with a certain degree of H3K4me1 signal, but barely with H3K27me3, suggesting that EGR1 functions primarily through promoter-proximal regions (Fig. 6f). EGR1 peaks were found at around 10,686 protein-coding genes. The majority of the differentially expressed genes have EGR1 peaks, as evidenced by 61.8% (1826/2956) of downregulated genes and 62.6% (1382/2209) of upregulated genes having EGR1 peaks (Fig. 6g). These findings suggest that EGR1 may either activate or repress gene transcription directly. In summary, EZH2 might govern a complex transcription program partly through the EGR1 silencer to regulate cell growth, death, migration, differentiation, and metabolism (Fig. 7).

Discussion

In this study, we developed an approach to systematically identify the TFs/chromatin-binding proteins regulating the expression of EZH2 and identified more than 20 such factors. We revealed reciprocal regulation of EGR1 and EZH2: EGR1 activates the expression of EZH2, and EZH2 represses EGR1 expression through a silencer downstream of the *EGR1* gene in breast cancer cells, in a PRC2 catalytic activity-dependent manner. Interestingly, our analysis suggests that the repression of EGR1 by EZH2 might be conserved in different cell types. The *EGR1* silencer region harbors high H3K27me3 and H3K4me1, and considerable H3K27ac and H3K4me3. To our knowledge, this is the first time that a region marked by such epigenetic settings has been shown to function as a silencer.

EGR1, as one of the immediate-early response genes, is involved in regulating cell growth and apoptosis [40, 51–54]. Importantly, EGR1 functions as a pro-differentiation factor in various contexts [55–62]. Owing to that EGR1 is highly expressed in normal breast tissues and potentially binds to most of the open chromatin region [63], fluctuation of EGR1 levels may therefore have an extensive impact on gene expression. Indeed, the increased expression of EGR1 after knocking out the *EGR1* silencer region resulted in changes in the expression of numerous genes in both MCF-7 and MDA-MB-231 cells, supporting a role for EGR1 in regulation of cell growth, cell death, differentiation, migration.

Significantly, our data suggested there are other intriguing facts about EGR1. For example, our data indicated that upregulation of EGR1 had complex effects on metabolism in the $EGR1^{+26\,kb}$ silencer-KO cells, notably resulting in downregulation of cholesterol biosynthetic

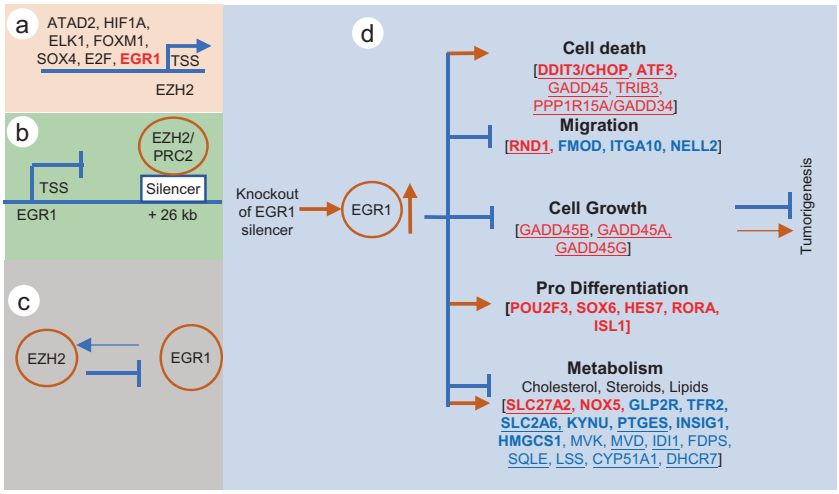

Fig. 7 Reciprocal regulation of EZH2 and EGR1 is implicated in breast tumorigenesis. a Multiple transcriptional factors (TFs) regulate the expression of EZH2, known TFs of EZH2 in breast cancers, including EGR1 which was identified in this research, are shown. **b** EZH2/PRC2 binds to the *EGR1* silencer, 26 kb downstream of *EGR1* transcription start site (TSS) and represses the expression of EGR1. **c** Dominance of EZH2 in the reciprocal regulation of EZH2 −EGR1 results in a negative correlation between the expression of EZH2 and EGR1. **d** EGR1 promotes or inhibits breast tumorigenesis through multiple direct/indirect downstream effectors: EGR1 activates the transcription of DDIT3/CHOP, ATF3, TRIB3, and PPP1R15A/GADD34 to promote apoptosis; EGR1 activates the transcription of GADD45B, GADD45A, and GADD45G to inhibit cell cycle; EGR1 could potentially inhibit migration through upregulation of RND1, and inhibition of FMOD, ITGA10, and NELL2; EGR1 upregulates transcriptional factors, such as POU2F3, SOX6, HES7, RORA, and ISL1, to promote differentiation, and inhibit tumorigenesis; EGR1 has a complex role in metabolism, including downregulation of genes encoding cholesterol biosynthesis pathway enzymes, which could potentially result in decreased production of cholesterol. Upregulated genes in cells after *EGR1* silencer knockout are indicated in red, downregulated genes in blue, genes with twofold change are noted in bold. Genes with EGR1 peaks in MCF-7 cells are underlined. *DDIT3* DNA-damage inducible transcript 3 *CHOP* C/EBP homologous protein; *ATF3* activating transcription factor 3; *TRIB3* tribbles pseudokinase 3; *PPP1R15A* protein phosphatase 1 regulatory subunit 15A; *GADD34* growth arrest and DNA-damage inducible 34; *RND1* rho family GTPase 1; *FMOD* fibromodulin; *ITGA10* integrin subunit alpha 10; *NELL2* neural EGFL Like 2; *GADD45B* growth arrest and DNA-damage inducible beta; *GADD45A* growth arrest and DNA-damage inducible alpha; *GADD45G* growth arrest and DNA-damage inducible gamma; *POU2F3* POU class 2 homeobox 3; *SOX6* SRY-Box transcription factor 6; *HES7* hes family BHLH transcription factor 7; *RORA* RAR related orphan receptor A; *ISL1* ISL LIM homeobox 1; *SLC27A2* solute carrier family 27 member 2; *NOX5* NADPH oxidase 5; *GLP2R* glucagon like peptide 2 receptor; *TFR2* transferrin receptor 2; *SLC2A6* solute carrier family 2 member 6; *KYNU* kynureninase; *PTGES* prostaglandin E synthase; *INSIG1* insulin induced gene 1; *HMGCS1* 3-hydroxy-3-methylglutaryl-CoA synthase 1; *MVK* mevalonate kinase; *MVD* mevalonate diphosphate decarboxylase; *IDI1* isopentenyl-diphosphate delta isomerase 1; *FDPS* farnesyl diphosphate synthase; *SQLE* squalene epoxidase; *LSS* lanosterol synthase; *CYP51A1* cytochrome P450 family 51 subfamily a member 1; *DHCR7* 7-dehydrocholesterol reductase.

genes, such as *HMGCS1*, *FDPS*, *IDI1*, *MVD*, *DHCR7*, *LSS,* and *SQLE*, which may decrease the production of cholesterol. The fact that similar results were seen in both MCF-7 and MDA-MB-231 cells suggests these observations are robust. However, a previous study reported conflicting results—EGR1 positively regulates cholesterol biosynthetic gene expression in liver [64]. Cholesterol metabolites can promote or suppress breast cancer [65, 66], indicating further work is needed to resolve these conflicting results and determine the involvement of EGR1 in cholesterol metabolism, and the role of cholesterol in breast cancer.

Our data also suggested the activation of DDIT3/CHOP mediated pathway in $EGR1^{+26\,kb}$ silencer-KO cells, as evidenced by increased expression of DDIT3/CHOP, PPP1R15A/GADD34, and TRIB3, the latter two are known targets of DDIT3/CHOP [46, 47]. DDIT3/CHOP, as a TF, controls genes encoding components involved in unfolded protein response and apoptosis [44, 45]. EGR1 and DDIT3 were often found to be coregulated together, but their relationship is not yet well understood. Our data suggested, for the first time, that DDIT3 is a direct target of EGR1. Also, our data indicate that upregulation of PPP1R15A/GADD34 and TRIB3 could be due to the combined effects of EGR1 and DDIT3. It is established that EGR1 could activate GADD45 [67], and GADD45 proteins were proposed to be central players in tumorigenesis [68]. They have multiple functions in blocking cell cycle progression, inducing apoptosis and promoting DNA repair, through interacting with proteins, such as CDK1, PCNA, MTK1, and CDKN1A [68–70]. Taken together, we suspect the upregulation of GADD45 and DDIT3 probably contributes significantly to the observed decrease in cell growth and tumorigenicity of the *EGR1* silencer-KO cells.

As summarized in Fig. 7, our study demonstrates that EZH2 overexpression in breast cancer occurs as the result of the dysregulation of multiple TFs, and EGR1 promotes the expression of EZH2 by binding to its promoter. Significantly, we found that EHZ2 brakes the expression of EGR1 through

a silencer region downstream of the *EGR1* gene, which in turn amplifies the regulatory effect of EZH2, resulting in changes in the expression of genes involved in cell growth, differentiation, death, migration, and metabolism. In light of these findings, we propose that the reciprocal regulation of EGR1 and EZH2 represents an important mechanism by which EHZ2 plays a role in tumorigenesis.

Materials and methods

Cell culture and reagents

MCF-7, MCF-10A, MDA-MB-231, and C2C12 cells were purchased from American Type Culture Collection. All cells were tested negative for mycoplasma contamination using the MycoAlert™ Mycoplasma Detection Kit (Lonza, Switzerland) and authenticated by short tandem repeat (STR) profiling (The University of Macau). All cells, except MCF-10A, were cultured in Dulbecco's modified Eagle's medium (Gibco, Thermo Fisher, Waltham, MA) with 10% fetal bovine serum (Gibco, Thermo Fisher) in 5% CO_2 at 37 °C. MCF-10A cells were cultured in DMEM supplemented with 10% FBS, 0.5 μg/mL hydrocortisone (Sigma-Aldrich, St. Louis, MO), 10 μg/mL insulin (Thermo Fisher), and 20 ng/mL hEGF (Thermo Fisher), and maintained in a 5% CO_2 incubator at 37 °C. The EZH2 inhibitor EPZ-6438 was purchased from Selleck Chemicals.

Details of additional methodologies can be found in Supplementary materials and methods. All the sgRNA sequences and primers used for cloning are listed in Supplementary Information, Table S4. The primers used for qRT-PCR can be found in Supplementary information, Table S5. The primary and secondary antibodies used are listed in Supplementary information, Table S6. Clinicopathological information for the tissue microarray_HBreD080CS01-3 (Shanghai Outdo Biotech, China) is listed in Supplementary Table S7.

Data availability

The RNA-seq data are deposited in the Gene Expression Omnibus (GEO) database under the accession number GSE134876.

Acknowledgements This work was funded by the Science and Technology Development Fund, Macau SAR (File no. 0107/2019/A2 and 095/2015/A3), the Science and Technology Program of Guangzhou, China (201807010101), and the Research & Development Administration Office of the University of Macau (MYRG201700099, MYRG2018-00022) awarded to GL.

Author contributions GL conceived and supervised the study. XG, HD, ZL, and YY carried out the experiments. XG, XZ, and GL analyzed data. ULC, YL, and JZ performed bioinformatic analysis. XW and GL drafted the paper. All authors have read and approved the paper.

Compliance with ethical standards

Conflict of interest The authors declare that they have no conflict of interest.

Publisher's note Springer Nature remains neutral with regard to jurisdictional claims in published maps and institutional affiliations.

References

1. Boyer LA, Plath K, Zeitlinger J, Brambrink T, Medeiros LA, Lee TI, et al. Polycomb complexes repress developmental regulators in murine embryonic stem cells. Nature. 2006;441:349–53.
2. Bracken AP, Dietrich N, Pasini D, Hansen KH, Helin K. Genome-wide mapping of Polycomb target genes unravels their roles in cell fate transitions. Genes Dev. 2006;20:1123–36.
3. Lee TI, Jenner RG, Boyer LA, Guenther MG, Levine SS, Kumar RM, et al. Control of developmental regulators by Polycomb in human embryonic stem cells. Cell. 2006;125:301–13.
4. Ernst T, Chase AJ, Score J, Hidalgo-Curtis CE, Bryant C, Jones AV, et al. Inactivating mutations of the histone methyltransferase gene EZH2 in myeloid disorders. Nat Genet. 2010;42:722–6.
5. Bejar R, Stevenson K, Abdel-Wahab O, Galili N, Nilsson B, Garcia-Manero G, et al. Clinical effect of point mutations in myelodysplastic syndromes. N Engl J Med. 2011;364:2496–506.
6. Varambally S, Dhanasekaran SM, Zhou M, Barrette TR, Kumar-Sinha C, Sanda MG, et al. The polycomb group protein EZH2 is involved in progression of prostate cancer. Nature. 2002;419:624–9.
7. Kleer CG, Cao Q, Varambally S, Shen R, Ota I, Tomlins SA, et al. EZH2 is a marker of aggressive breast cancer and promotes neoplastic transformation of breast epithelial cells. Proc Natl Acad Sci USA. 2003;100:11606–11.
8. Breuer RH, Snijders PJ, Smit EF, Sutedja TG, Sewalt RG, Otte AP, et al. Increased expression of the EZH2 polycomb group gene in BMI-1-positive neoplastic cells during bronchial carcinogenesis. Neoplasia. 2004;6:736–43.
9. Sudo T, Utsunomiya T, Mimori K, Nagahara H, Ogawa K, Inoue H, et al. Clinicopathological significance of EZH2 mRNA expression in patients with hepatocellular carcinoma. Br J Cancer. 2005;92:1754–8.
10. Weikert S, Christoph F, Kollermann J, Muller M, Schrader M, Miller K, et al. Expression levels of the EZH2 polycomb transcriptional repressor correlate with aggressiveness and invasive potential of bladder carcinomas. Int J Mol Med. 2005;16:349–53.
11. Bachmann IM, Halvorsen OJ, Collett K, Stefansson IM, Straume O, Haukaas SA, et al. EZH2 expression is associated with high proliferation rate and aggressive tumor subgroups in cutaneous melanoma and cancers of the endometrium, prostate, and breast. J Clin Oncol. 2006;24:268–73.
12. Wagener N, Macher-Goeppinger S, Pritsch M, Husing J, Hoppe-Seyler K, Schirmacher P, et al. Enhancer of zeste homolog 2 (EZH2) expression is an independent prognostic factor in renal cell carcinoma. BMC Cancer. 2010;10:524.
13. Takawa M, Masuda K, Kunizaki M, Daigo Y, Takagi K, Iwai Y, et al. Validation of the histone methyltransferase EZH2 as a therapeutic target for various types of human cancer and as a prognostic marker. Cancer Sci. 2011;102:1298–305.
14. Gnad F, Doll S, Manning G, Arnott D, Zhang Z. Bioinformatics analysis of thousands of TCGA tumors to determine the involvement of epigenetic regulators in human cancer. BMC Genom. 2015;16 Suppl 8:S5.

15. Saramaki OR, Tammela TL, Martikainen PM, Vessella RL, Visakorpi T. The gene for polycomb group protein enhancer of zeste homolog 2 (EZH2) is amplified in late-stage prostate cancer. Genes Chromosomes Cancer. 2006;45:639–45.
16. Koh CM, Iwata T, Zheng Q, Bethel C, Yegnasubramanian S, De Marzo AM. Myc enforces overexpression of EZH2 in early prostatic neoplasia via transcriptional and post-transcriptional mechanisms. Oncotarget. 2011;2:669–83.
17. Bracken AP, Pasini D, Capra M, Prosperini E, Colli E, Helin K. EZH2 is downstream of the pRB-E2F pathway, essential for proliferation and amplified in cancer. EMBO J. 2003;22:5323–35.
18. Oeggerli M, Tomovska S, Schraml P, Calvano-Forte D, Schafroth S, Simon R, et al. E2F3 amplification and overexpression is associated with invasive tumor growth and rapid tumor cell proliferation in urinary bladder cancer. Oncogene. 2004;23:5616–23.
19. Lin Y-W, Ren L-L, Xiong H, Du W, Yu Y-N, Sun T-T, et al. Role of STAT3 and vitamin D receptor in EZH2 -mediated invasion of human colorectal cancer. J Pathol. 2013;230:277–90.
20. Varambally S, Cao Q, Mani RS, Shankar S, Wang X, Ateeq B, et al. Genomic loss of microRNA-101 leads to overexpression of histone methyltransferase EZH2 in cancer. Science. 2008;322:1695–9.
21. Ciarapica R, Russo G, Verginelli F, Raimondi L, Donfrancesco A, Rota R, et al. Deregulated expression of miR-26a and Ezh2 in rhabdomyosarcoma. Cell Cycle. 2009;8:172–5.
22. Alajez NM, Shi W, Hui AB, Bruce J, Lenarduzzi M, Ito E, et al. Enhancer of Zeste homolog 2 (EZH2) is overexpressed in recurrent nasopharyngeal carcinoma and is regulated by miR-26a, miR-101, and miR-98. Cell Death Dis. 2010;1:e85.
23. Yamaguchi H, Hung M-C. Regulation and role of EZH2 in cancer. Cancer Res Treat. 2014;46:209–22.
24. Wang GG, Konze KD, Tao J. Polycomb genes, miRNA, and their deregulation in B-cell malignancies. Blood. 2015;125:1217–25.
25. Mahara S, Lee PL, Feng M, Tergaonkar V, Chng WJ, Yu Q. HIFI-alpha activation underlies a functional switch in the paradoxical role of Ezh2/PRC2 in breast cancer. Proc Natl Acad Sci USA. 2016;113:E3735–44.
26. Chang C-J, Yang J-Y, Xia W, Chen C-T, Xie X, Chao C-H, et al. EZH2 promotes expansion of breast tumor initiating cells through activation of RAF1-β-catenin signaling. Cancer Cell. 2011;19:86–100.
27. Fujii S, Tokita K, Wada N, Ito K, Yamauchi C, Ito Y, et al. MEK-ERK pathway regulates EZH2 overexpression in association with aggressive breast cancer subtypes. Oncogene. 2011;30:4118–28.
28. Tiwari N, Tiwari Vijay K, Waldmeier L, Balwierz Piotr J, Arnold P, Pachkov M, et al. Sox4 is a master regulator of epithelial-mesenchymal transition by controlling Ezh2 expression and epigenetic reprogramming. Cancer Cell. 2013;23:768–83.
29. Kalashnikova EV, Revenko AS, Gemo AT, Andrews NP, Tepper CG, Zou JX, et al. ANCCA/ATAD2 overexpression identifies breast cancer patients with poor prognosis, acting to drive proliferation and survival of triple-negative cells through control of B-Myb and EZH2. Cancer Res. 2010;70:9402–12.
30. McCabe MT, Creasy CL. EZH2 as a potential target in cancer therapy. Epigenomics. 2014;6:341–51.
31. Koppens M, van Lohuizen M. Context-dependent actions of Polycomb repressors in cancer. Oncogene. 2016;35:1341–52.
32. Kotake Y, Cao R, Viatour P, Sage J, Zhang Y, Xiong Y. pRB family proteins are required for H3K27 trimethylation and Polycomb repression complexes binding to and silencing p16INK4alpha tumor suppressor gene. Genes Dev. 2007;21:49–54.
33. Cao Q, Yu J, Dhanasekaran SM, Kim JH, Mani RS, Tomlins SA, et al. Repression of E-cadherin by the polycomb group protein EZH2 in cancer. Oncogene. 2008;27:7274–84.
34. Du J, Li L, Ou Z, Kong C, Zhang Y, Dong Z, et al. FOXC1, a target of polycomb, inhibits metastasis of breast cancer cells. Breast Cancer Res Treat. 2012;131:65–73.
35. Wassef M, Margueron R. The multiple facets of PRC2 alterations in cancers. J Mol Biol. 2017;429:1978–93.
36. Zeng J, Li G. TFmapper: a tool for searching putative factors regulating gene expression using ChIP-seq data. Int J Biol Sci. 2018;14:1724–31.
37. Zheng R, Wan C, Mei S, Qin Q, Wu Q, Sun H, et al. Cistrome Data Browser: expanded datasets and new tools for gene regulatory analysis. Nucleic Acids Res. 2019;47:D729–35.
38. Mei S, Qin Q, Wu Q, Sun H, Zheng R, Zang C, et al. Cistrome Data Browser: a data portal for ChIP-Seq and chromatin accessibility data in human and mouse. Nucleic Acids Res. 2017;45:D658–62.
39. Baron V, Adamson ED, Calogero A, Ragona G, Mercola D. The transcription factor Egr1 is a direct regulator of multiple tumor suppressors including TGF beta 1, PTEN, p53, and fibronectin. Cancer Gene Ther. 2006;13:115–24.
40. Pagel J-I, Deindl E. Early growth response 1-A transcription factor in the crossfire of signal transduction cascades. Indian J Biochem Biophys. 2011;48:226–35.
41. Khan A, Fornes O, Stigliani A, Gheorghe M, Castro-Mondragon JA, van der Lee R, et al. JASPAR 2018: update of the open-access database of transcription factor binding profiles and its web framework. Nucleic Acids Res. 2018;46:D1284.
42. Liu C, Rangnekar VM, Adamson E, Mercola D. Suppression of growth and transformation and induction of apoptosis by EGR-1. Cancer Gene Ther. 1998;5:3–28.
43. Silverman ES, Du J, Williams AJ, Wadgaonkar R, Drazen JM, Collins T. cAMP-response-element-binding-protein-binding protein (CBP) and p300 are transcriptional co-activators of early growth response factor-1 (Egr-1). Biochem J. 1998;336:183–9.
44. Hetz C, Zhang K, Kaufman RJ. Mechanisms, regulation and functions of the unfolded protein response. Nat Rev Mol Cell Biol. 2020;21:421–38.
45. Walter P, Ron D. The unfolded protein response: from stress pathway to homeostatic regulation. Science. 2011;334:1081–6.
46. Marciniak SJ, Yun CY, Oyadomari S, Novoa I, Zhang YH, Jungreis R, et al. CHOP induces death by promoting protein synthesis and oxidation in the stressed endoplasmic reticulum. Genes Dev. 2004;18:3066–77.
47. Ohoka N, Yoshii S, Hattori T, Onozaki K, Hayashi H. *TRB3*, a novel ER stress-inducible gene, is induced via ATF4-CHOP pathway and is involved in cell death. Embo J. 2005;24:1243–55.
48. Nobes CD, Lauritzen I, Mattei MG, Paris S, Hall A, Chardin P. A new member of the Rho family, Rnd1, promotes disassembly of actin filament structures and loss of cell adhesion. J Cell Biol. 1998;141:187–97.
49. Okada T, Sinha S, Esposito I, Schiavon G, López-Lago MA, Su W, et al. The Rho GTPase Rnd1 suppresses mammary tumorigenesis and EMT by restraining Ras-MAPK signalling. Nat Cell Biol. 2015;17:81–94.
50. Tanaka S, Miyagi S, Sashida G, Chiba T, Yuan J, Mochizuki-Kashio M, et al. Ezh2 augments leukemogenicity by reinforcing differentiation blockage in acute myeloid leukemia. Blood. 2012;120:1107–17.
51. Bahrami S, Drabløs F. Gene regulation in the immediate-early response process. Adv Biol Regul. 2016;62:37–49.
52. Thiel G, Cibelli G. Regulation of life and death by the zinc finger transcription factor Egr-1. J Cell Physiol. 2002;193:287–92.
53. Yu J, Baron V, Mercola D, Mustelin T, Adamson ED. A network of p73, p53 and Egr1 is required for efficient apoptosis in tumor cells. Cell Death Differ. 2007;14:436–46.
54. Bhattacharyya S, Fang F, Tourtellotte W, Varga J. Egr-1: new conductor for the tissue repair orchestra directs harmony (regeneration) or cacophony (fibrosis). J Pathol. 2013;229:286–97.
55. Sukhatme VP, Cao XM, Chang LC, Tsai-Morris CH, Stamenkovich D, Ferreira PC, et al. A zinc finger-encoding gene

coregulated with c-fos during growth and differentiation, and after cellular depolarization. Cell. 1988;53:37–43.
56. Nguyen HQ, Hoffman-Liebermann B, Liebermann DA. The zinc finger transcription factor Egr-1 is essential for and restricts differentiation along the macrophage lineage. Cell. 1993;72:197–209.
57. Barbieri E, Trizzino M, Welsh SA, Owens TA, Calabretta B, Carroll M, et al. Targeted enhancer activation by a subunit of the integrator complex. Mol Cell. 2018;71:103–16.e7.
58. Lejard V, Blais F, Guerquin MJ, Bonnet A, Bonnin MA, Havis E, et al. EGR1 and EGR2 involvement in vertebrate tendon differentiation. J Biol Chem. 2011;286:5855–67.
59. Spaapen F, van den Akker GG, Caron MM, Prickaerts P, Rofel C, Dahlmans VE, et al. The immediate early gene product EGR1 and polycomb group proteins interact in epigenetic programming during chondrogenesis. PLoS One. 2013;8:e58083.
60. Worringer KA, Rand TA, Hayashi Y, Sami S, Takahashi K, Tanabe K, et al. The let-7/LIN-41 pathway regulates reprogramming to human induced pluripotent stem cells by controlling expression of prodifferentiation genes. Cell Stem Cell. 2014;14:40–52.
61. Gibbs JD, Liebermann DA, Hoffman B. Egr-1 abrogates the E2F-1 block in terminal myeloid differentiation and suppresses leukemia. Oncogene. 2008;27:98–106.
62. Shafarenko M, Liebermann DA, Hoffman B. Egr-1 abrogates the block imparted by c-Myc on terminal M1 myeloid differentiation. Blood. 2005;106:871–8.
63. Keilwagen J, Posch S, Grau J. Accurate prediction of cell type-specific transcription factor binding. Genome Biol. 2019;20:9.
64. Gokey NG, Lopez-Anido C, Gillian-Daniel AL, Svaren J. Early growth response 1 (Egr1) regulates cholesterol biosynthetic gene expression. J Biol Chem. 2011;286:29501–10.
65. Kuzu OF, Noory MA, Robertson GP. The role of cholesterol in cancer. Cancer Res. 2016;76:2063–70.
66. Silvente-Poirot S, Poirot M. Cancer. Cholesterol and cancer, in the balance. Science. 2014;343:1445–6.
67. Thyss R, Virolle V, Imbert V, Peyron JF, Aberdam D, Virolle T. NF-kappaB/Egr-1/Gadd45 are sequentially activated upon UVB irradiation to mediate epidermal cell death. EMBO J. 2005;24:128–37.
68. Tamura RE, de Vasconcellos JF, Sarkar D, Libermann TA, Fisher PB, Zerbini LF. GADD45 proteins: central players in tumorigenesis. Curr Mol Med. 2012;12:634–51.
69. Pietrasik S, Zajac G, Morawiec J, Soszynski M, Fila M, Blasiak J. Interplay between BRCA1 and GADD45A and its potential for nucleotide excision repair in breast cancer pathogenesis. Int J Mol Sci. 2020;21:870.1–22.
70. Salvador JM, Brown-Clay JD, Fornace AJ Jr. Gadd45 in stress signaling, cell cycle control, and apoptosis. Adv Exp Med Biol. 2013;793:1–19.